Calculating the hydraulic inductance of a compressor duct

Calculating the Hydraulic Inductance of a Compressor Duct

J. van Helvoirt

DCT 2006.10

DCT Internal report

Co-supervisor: B. de Jager

Supervisor: M. Steinbuch

Technische Universiteit Eindhoven
Department Mechanical Engineering
Dynamics and Control Technology Group

Eindhoven, January, 2006

Abstract

The Greitzer model is a well-known nonlinear model that describes the transient behavior of compression systems. The model is particularly useful for describing the limit cycle oscillations associated with a compressor instability called surge.

One of the important parameters in the model is the so-called hydraulic inductance. With an appropriate choice of this parameter, all the kinetic energy of the flow through the compressor is lumped onto a duct of a certain length and with a constant cross-sectional area. The actual value for the hydraulic inductance is usually determined by tuning the Greitzer model to obtain a good match between measured and simulated surge oscillations.

In this report we propose a different way to determine the hydraulic inductance for a compressor duct. After various geometric simplifications, the governing integral of the cross-sectional duct area along the entire flow path, is calculated directly.

The values for the hydraulic inductance of two compressor test rigs are determined. When comparing the result for one rig with a tuned inductance value, a large difference can be observed. This difference might indicate that not all the relevant dynamic effects are captured by the lumped Greitzer model.

1 Introduction

The operating range of turbo compressors is limited towards low mass flows by the occurrence of surge and rotating stall. Surge is an unstable operating mode of a compression system, characterized by large oscillations in compressor flow and pressure rise. Surge reduces compressor performance and the resulting thermal and mechanical loads can cause structural damage.

One of the first nonlinear models of transient compressor behavior was proposed in [1]. This model is capable of describing the limit cycle oscillations in compressor flow and pressure rise that are associated with surge. Although developed for axial compressors, the authors of [2] showed that this nonlinear model was also applicable to centrifugal compressors. To this day, it is the most widely used dynamic model in the field.

The main idea of the approach used in [1] is to associate the kinetic and potential energy of the compressor transients with different components of the compression system. Therefore, in the derivation of the Greitzer model the fluid dynamics in the compressor and the connecting ducts are accounted for by a constant area pipe of a certain length. The pressure rise due to the compressor is represented by an actuator disk. Similarly, the duct in which the throttle resides is modeled by a second constant area pipe and actuator disk.

In the Greitzer model the parameter L/A appears in the momentum equation for both the compressor and throttle ducts. This parameter is usually referred to as the hydraulic inductance. In practice the momentum equation for the throttle duct can usually be neglected, see for example [3, 4]. In contrast, the hydraulic inductance of the compressor duct L_c/A_c plays an important role in describing the dynamic behavior of the compression system.

However, we point out that the parameter L_c/A_c is already a simplification for the actual term in the momentum equation, namely

$$\int\limits_{\substack{actual\\ducting}} \frac{ds}{A(s)} = \left(\frac{L_c}{A_c}\right)_{model} \tag{1}$$

This relation implies that the actual duct is replaced by a constant area pipe of a certain length to obtain a simple expression for the hydraulic inductance L_c/A_c. However, in practice the area of the compressor duct is not constant, so the corresponding duct length L_c must be determined iteratively.

In order to avoid tuning of the duct length L_c, we propose to calculate the integral of the duct area $A(s)$ along the flow path s directly. Due to the complex three-dimensional geometry of the internals of a centrifugal compressors, we divide the total duct into several sections and apply appropriate assumptions to solve the integral for each of those sections. The method will be evaluated on two different compressor configurations and after a short discussion of the results we finish with some concluding remarks.

2 Calculating the hydraulic inductance

In Figure 1 the cross section is shown for a typical configuration of a centrifugal compressor. From this figure we observe a distinct reduction of the cross-sectional area along the direction of flow. These area changes define the start and end point of the compressor duct. Following the geometry of the compressor internals, a partitioning of the total duct into various elements is suggested, according to Figure 2. We point out that the impeller is subdivided into a curved duct and a radial duct. We will now present analytical approximations of the integral in (1) for each of the simplified geometries and the assumptions that were made during the derivations.

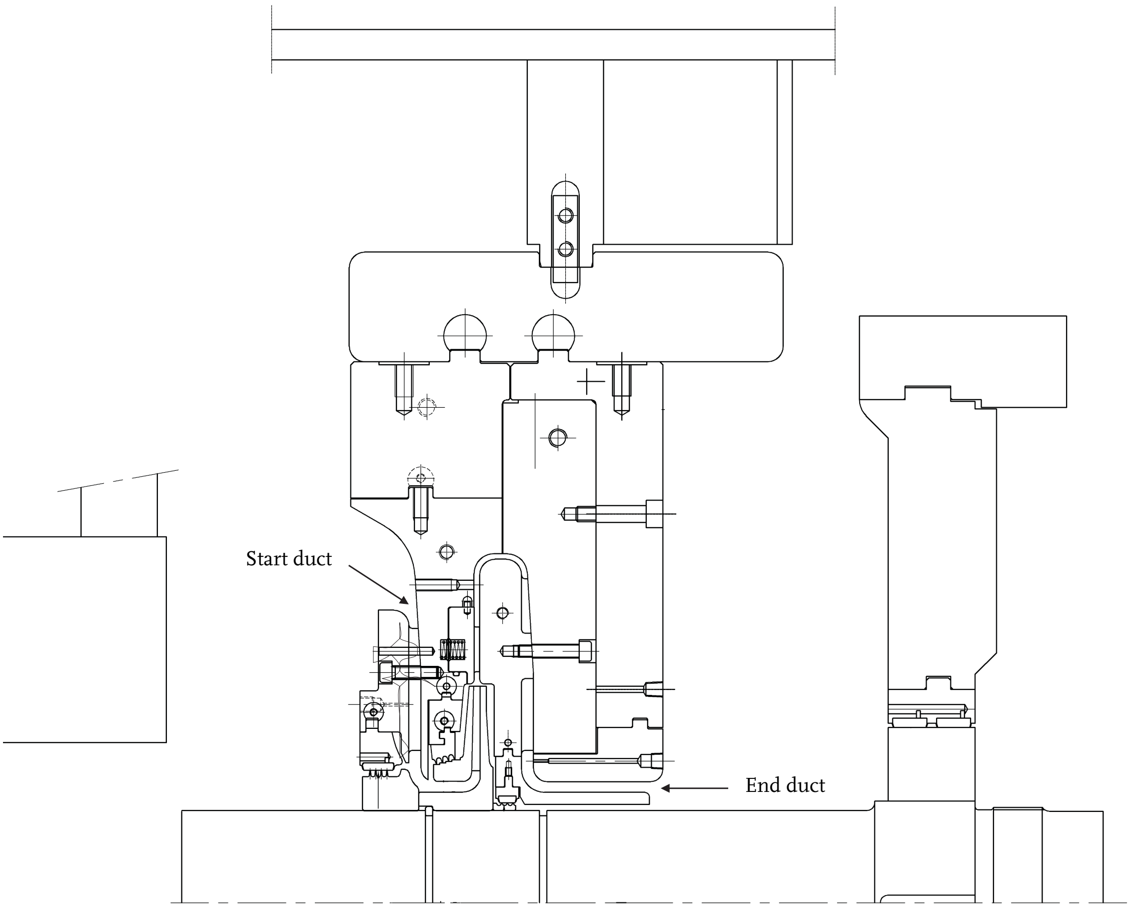

Figure 1: Cross sectional view of a typical configuration for a centrifugal compressor.

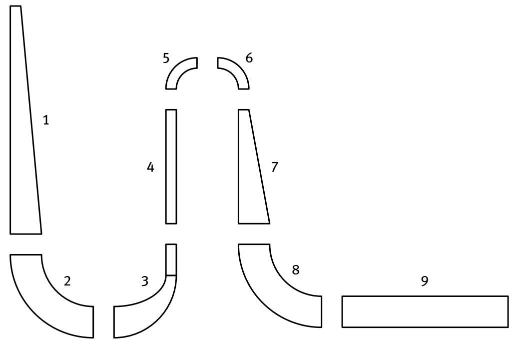

Nr.	Description	Geometry
1	inlet channel	diverging radial duct
2	inlet bend	curved duct, type A
3	impeller	curved duct, type B
"	"	radial duct
4	diffuser	radial duct
5	diffuser bend	curved duct, type C
6	diffuser bend	curved duct, type D
7	return channel	diverging radial duct
8	return bend	curved duct, type A
9	outlet channel	axial duct

Figure 2: Division of compressor ducting into elements with simple geometry.

2.1 Straight radial ducts

Following the geometry from Figure 3 the following expression for the hydraulic inductance is obtained

$$\int_{\mathcal{S}} \frac{ds}{A(s)} = \int_{y_1}^{y_2} \frac{dy}{2\pi w y} = \begin{cases} \frac{1}{2\pi w} \ln\left(\frac{y_2}{y_1}\right) & \text{for} \quad y_2 > y_1 > 0 \\ -\frac{1}{2\pi w} \ln\left(\frac{y_2}{y_1}\right) & \text{for} \quad y_1 > y_2 > 0 \end{cases} \tag{2}$$

where we assume that $ds = dy$, requiring that the flow through the duct is strictly radial and uniform.

2.2 Diverging radial ducts

Following the geometry from Figure 4 the following expression for the hydraulic inductance is obtained

$$\int_{\mathcal{S}} \frac{ds}{A(s)} = \int_{y_1}^{y_2} \frac{dy}{2\pi w(y) y} = \begin{cases} \frac{1}{2\pi b} \ln\left(\frac{y_2(ay_1+b)}{y_1(ay_2+b)}\right) & \text{for} \quad y_2 w(y_1) > y_1 w(y_2) > 0 \\ -\frac{1}{2\pi b} \ln\left(\frac{y_2(ay_1+b)}{y_1(ay_2+b)}\right) & \text{for} \quad y_1 w(y_2) > y_2 w(y_1) > 0 \end{cases} \tag{3}$$

where we assume that $ds = dy$, requiring that the flow through the duct is strictly radial and uniform. Furthermore, we assume a linearly increasing or decreasing width of the duct, yielding the following expression for $w(y)$

$$w(y) = ay + b = \underbrace{\frac{w_2 - w_1}{y_2 - y_1}}_{a} y + \underbrace{w_1 - \frac{w_2 - w_1}{y_2 - y_1} y_1}_{b} \tag{4}$$

2.3 Straight axial ducts

Following the geometry from Figure 5 the following expression for the hydraulic inductance is obtained

$$\int_{\mathcal{S}} \frac{ds}{A(s)} = \int_{x_1}^{x_2} \frac{dx}{\pi(y_1 + y_2) w} = \frac{|x_2 - x_1|}{\pi(y_1 + y_2) w} \tag{5}$$

where we assume that $ds = dx$, requiring that the flow through the duct is strictly axial and uniform.

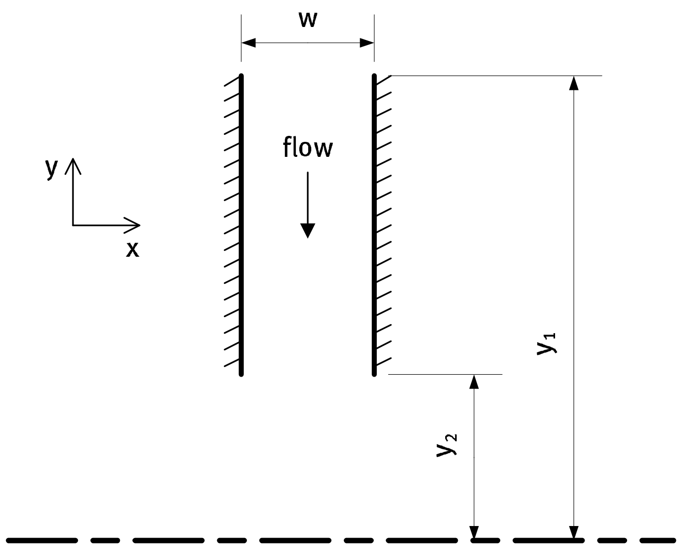

Figure 3: Radial duct geometry.

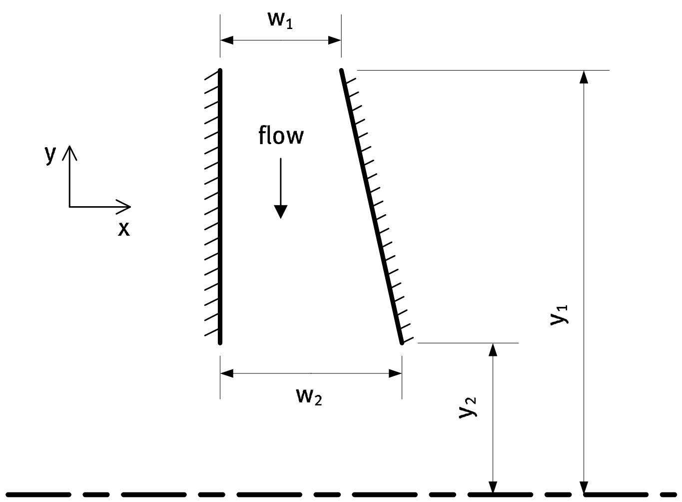

Figure 4: Diverging radial duct geometry.

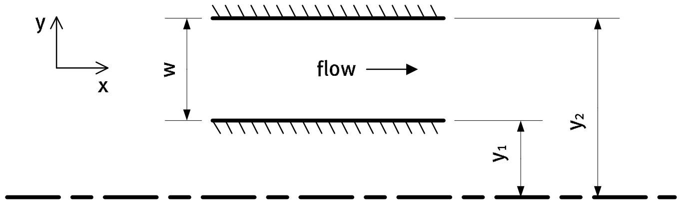

Figure 5: Axial duct geometry.

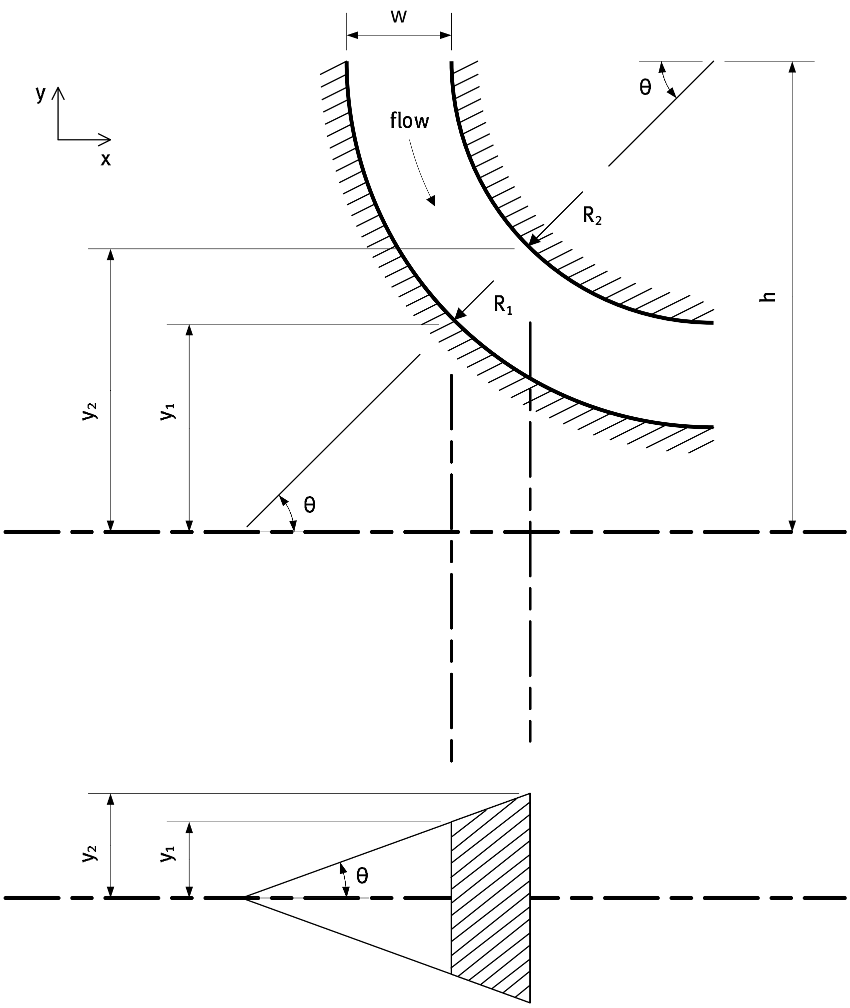

Figure 6: Curved duct geometry, type A.

2.4 Curved ducts

For the various bends in the compressor duct we make use of an auxiliary geometry as shown in Figure 6. From this figure we see that the cross sectional area of the duct at an angle θ is given by the lateral area of the frustum $A(\theta) = \pi w(y_1(\theta) + y_2(\theta))$ with $y_i = h - R_i \sin\theta$, $i = 1, 2$.

Following the geometry from Figure 5 the following expression for the hydraulic inductance is obtained

$$\int_{\mathcal{S}} \frac{ds}{A(s)} = \int_0^{\phi} \frac{\frac{1}{2}(R_1 + R_2)}{A(\theta)} d\theta = \frac{R_1 + R_2}{\pi w \sqrt{4h^2 - (R_1 + R_2)^2}} \tan^{-1}\left(\frac{-R_1 - R_2 + 2h\tan(\frac{\theta}{2})}{\sqrt{4h^2 - (R_1 + R_2)^2}}\right) \quad (6)$$

where we assume that $ds = \frac{1}{2}(R_1 + R_2)d\theta$, requiring that the flow is uniform and that it follows the centerline of the curved duct from Figure 6. Note that ϕ denotes the angle in rad at the end of the curved duct.

Analogous to this approach, expressions for the curved ducts of type B, C, and D can be obtained. However, note that the resulting expressions are different due to the start and end position of the ducts relative to the flow.

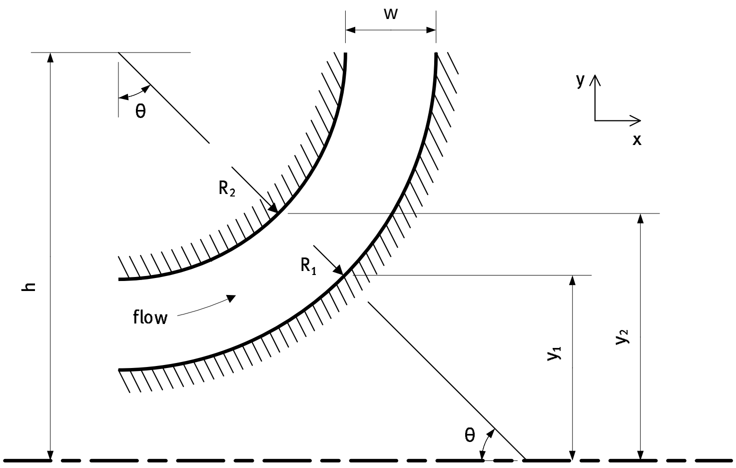

Figure 7: Curved duct geometry, type B.

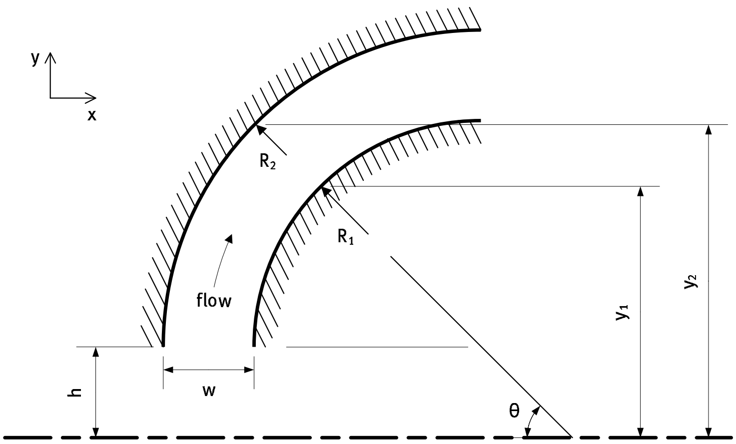

Figure 8: Curved duct geometry, type C.

Following the geometry from Figure 7 the following expression for the hydraulic inductance for a curved duct of type B is obtained

$$\int_{\mathcal{S}} \frac{ds}{A(s)} = \frac{R_1 + R_2}{\pi w \sqrt{(R_1+R_2)^2 - 4h^2}} \tanh^{-1}\left(\frac{(R_1+R_2+2h)\tan(\frac{\theta}{2})}{\sqrt{(R_1+R_2)^2-4h^2}}\right) \tag{7}$$

using $y_i = h - R_i \cos\theta$, while the hydraulic inductance for a curved duct of type C (see Figure 8) is given by

$$\int_{\mathcal{S}} \frac{ds}{A(s)} = \frac{R_1 + R_2}{\pi w \sqrt{4h^2 - (R_1+R_2)^2}} \tan^{-1}\left(\frac{R_1+R_2+2h\tan(\frac{\theta}{2})}{\sqrt{4h^2-(R_1+R_2)^2}}\right) \tag{8}$$

using $y_i = h + R_i \sin\theta$. Finally, the hydraulic inductance for a curved duct of type D (see Figure 9)is given by

$$\int_{\mathcal{S}} \frac{ds}{A(s)} = \frac{R_1 + R_2}{\pi w \sqrt{(R_1+R_2)^2 - 4h^2}} \tanh^{-1}\left(\frac{(R_1+R_2-2h)\tan(\frac{\theta}{2})}{\sqrt{(R_1+R_2)^2-4h^2}}\right) \tag{9}$$

using $y_i = h + R_i \cos\theta$.

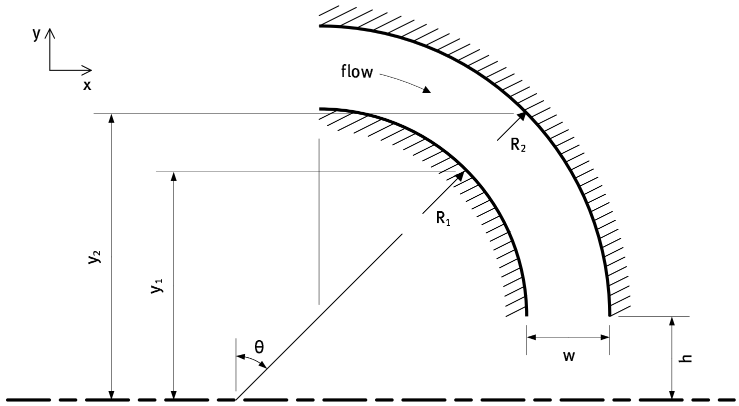

Figure 9: Curved duct geometry, type D.

3 Numerical results and validation

We have developed expressions for the hydraulic inductance of each element of the compressor duct. With these approximations we will now calculate the hydraulic inductance for the total compressor ducts of two single stage compressor test rigs. The geometry of the test rig of Siemens Power Generation and Industrial Applications in Hengelo, The Netherlands is given in Figure ??. Data for the second test rig of Siemens in Duisburg, Germany are confidential and hence not included in this report.

The calculation results for the test rig in Hengelo with impeller type RD7038-50EB1 are given in the third column of Table 1. The value for the hydraulic inductance L_c/A_c is obtained by summing the values for the individual components, yielding $L_c/A_c = 35.3\ \mathrm{m}^{-1}$.

For comparison we also determined the hydraulic inductance by the commonly used method of matching simulated surge frequency and amplitude with measured values. For this purpose a reference area A_c^* was selected and the duct length L_c was obtained by tuning the Greitzer model, yielding $L_c^*/A_c^* = 92.9\ \mathrm{m}^{-1}$. Note that a large difference exists between the calculated and tuned values for the hydraulic inductance. Therefore, another dynamic effect should be incorporated in the model to adjust for the observed differences between model and experiment when L_c is determined according to the method described here. Suggestions to solve this problem are given in for example [2, 5].

Calculations were also performed for the test rig in Duisburg with the LR-65EA1 impeller and the results are given in the last column of Table 1. We point out that for this test rig the inlet channel has a constant width. The resulting value for the total hydraulic inductance is $L_c/A_c = 30.8\ \mathrm{m}^{-1}$. So far no comparison can be made with the tuned value for the hydraulic inductance on this test rig since experimental data is not yet available.

Finally, we point out that the suggested geometries in Figure 2 are simplifications of the actual compressor geometry. In particular, representing the impeller by a $90\,\mathrm{deg}$ bend and a radial duct results in a drastic simplification of the impeller geometry with its curved blades. A more detailed (numerical) calculation of the integral in (1) could provide more insight in the validity of the geometric simplifications. However, given the relatively small contribution ($\simeq$ 10–17 %) of the impeller on the total inductance value, it is unlikely that more accurate integration will lead to a better agreement between calculated and tuned values for the hydraulic inductance.

Table 1: Hydraulic inductance calculation for both test rigs.

Number	**Duct type**	L_c/A_c	
		50EB1	65EA1
1	inlet channel	5.62	3.55
2	inlet bend	2.61	2.11
3	impeller bend	2.61	2.11
"	impeller duct	3.37	1.10
4	diffuser	6.44	5.37
5	diffuser bend	1.00	1.38
6	diffuser bend	0.986	1.38
7	return channel	7.68	4.29
8	return bend	2.98	1.86
9	outlet channel	1.99	7.69
sum	total channel	35.3	30.8

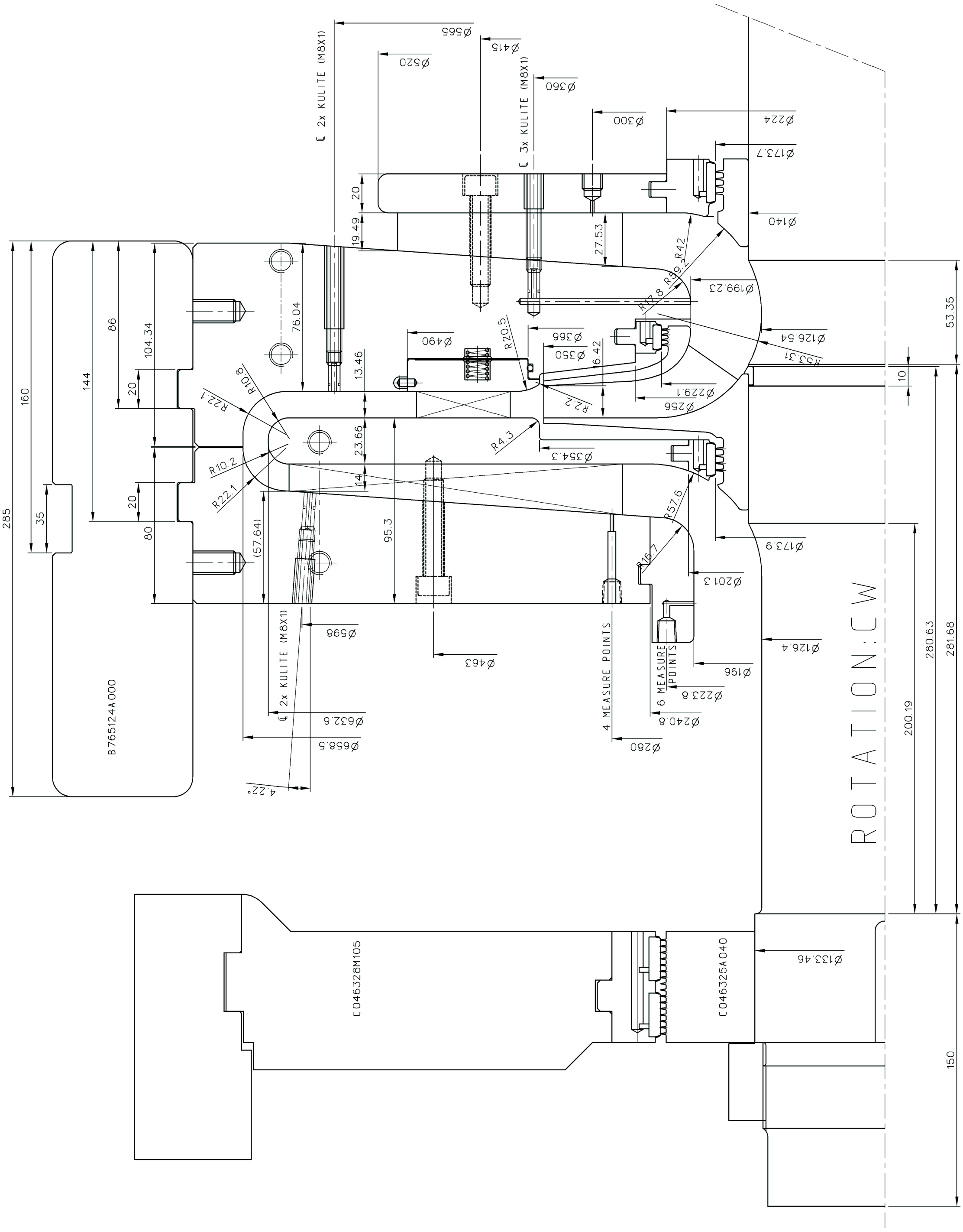

Figure 10: Geometry and dimensions of test rig in Hengelo with impeller 50EB1.

References

[1] E. M. Greitzer, "Surge and rotating stall in axial flow compressors: Part I—Theoretical compression system model," *ASME J. Eng. Power*, vol. 98, pp. 190–198, 1976.

[2] K. E. Hansen, P. Jørgensen, and P. S. Larsen, "Experimental and theoretical study of surge in a small centrifugal compressor," *ASME J. Fluids Eng.*, vol. 103, pp. 391–395, 1981.

[3] F. P. T. Willems, "Modeling and bounded feedback stabilization of centrifugal compressor surge," Ph.D. dissertation, Technische Universiteit Eindhoven, Eindhoven, The Netherlands, 2000, online available at: http://alexandria.tue.nl/extra2/200011493.pdf.

[4] J. van Helvoirt, B. de Jager, M. Steinbuch, and J. Smeulers, "Stability parameter identification for a centrifugal compression system," in *Proc. 43rd IEEE Conf. on Decision and Control*, Atlantis, Paradise Island, Bahamas, 2004, pp. 3400–3405.

[5] C. H. J. Meuleman, "Measurement and unsteady flow modelling of centrifugal compressor surge," Ph.D. dissertation, Technische Universiteit Eindhoven, Eindhoven, The Netherlands, 2002, online available at: http://alexandria.tue.nl/extra2/200213364.pdf.